Graphene oxide used as the modifier to prepare silica-encapsulated waterborne flaky aluminium for enhanced anticorrosive property

Liqi Liu, Kaiqin Shi, Yilin Lu, Chengbing Yu ✉

School of Materials Science and Engineering, Shanghai University, Shanghai 200444, People's Republic of China
✉ *E-mail: ycb101@shu.edu.cn*

Published in Micro & Nano Letters; Received on 1st May 2020; Revised on 21st May 2020; Accepted on 31st May 2020

Silica-encapsulated waterborne flaky aluminium (SEWFA) is widely used in industrial fields, but its corrosion hampers its long-term use. Herein, a sol–gel method was used to prepare graphene oxide (GO)-modified SEWFA (GO-SEWFA). The oxygen-containing functional groups of GO can react with tetraethyl orthosilicate to form a well-dispersed silica/GO matrix on the surface of GO-SEWFA. The hydrogen evolution results demonstrated that GO covalent bonding, combined with silica encapsulation on the surface of flaky aluminium, could effectively improve the anticorrosive performance.

1. Introduction: Flaky aluminium is widely used in industrial production due to its special metal and glossy properties, especially in inks, plastics, furniture manufacturing, automotive paint and marine coatings. However, flaky aluminium suffers from a highly reactive chemical surface, so it is necessary to modify the surface to enhance its corrosion resistance [1, 2]. Numerous techniques exist that include inorganic coating [3, 4], organic coating [5] and organic–inorganic hybrid coating [6, 7]. Encapsulation with silica to form a stable core–shell structure has shown to be one of the most practical and stable surface modifications [8, 9].

Earlier work has identified the mechanisms underlying the enhanced anticorrosive properties of silica-capped aluminium powders [10]. Kiehl and Brendel [11] argued that the mechanism of aluminium pigments can be divided into two categories: reducing active sites and forming a physical barrier. The main principle is that active silica reacts with hydroxyl groups on the surface of aluminium pigments to form a physical barrier against surface corrosion media. Additionally, the hydroxyl-silica reaction reduces the active sites of corrosion reaction of aluminium pigments.

Graphene has found many applications in corrosion-resistance coatings since it can also act as a barrier to the outside environment [12–14]. However, its dispersion compatibility, high cost and strong van der Waals forces limit its large-scale applications [15]. Many works have focused on modification techniques to improve the mixing properties of graphene [16, 17]. Given the rich surface oxygen-containing functional groups, few-layer graphene oxide (GO) can improve the performance of a silica-based coating to further protect the flaky aluminium. As such, an approach to couple GO with encapsulated flaky aluminium has first been developed here for enhanced the anticorrosive property of silica-encapsulated waterborne flaky aluminium (SEWFA). By adding GO, a new type of SEWFA is formed through a covalently cross-linked network structure between GO and silica. The anticorrosive property of GO-modified SEWFA (GO-SEWFA) was evaluated by hydrogen evolution test, and the surface morphology and anticorrosive mechanism were analysised.

2. Experimental details

2.1. Materials: Flaky aluminium powder was kindly provided by Pancai Metal Pigment Co., Ltd (Shanghai, China). Tetraethyl orthosilicate (TEOS) was provided by Jiuhuan New Materials Technology Co., Ltd. (Changzhou, China). Anhydrous ethanol, ammonia, acetone were of analytical reagent and provided by Sinopharm Group Chemical Reagent Co., Ltd (Shanghai, China). GO was prepared with the improved Hummer's method (Appendix).

2.2. Preparation of GO-SEWFA: The GO product was diluted with distilled water to a concentration of 0.34 wt%. Initially, 7.5 g of GO solution was added to 20 mL anhydrous ethanol, and ultrasonically dispersed for 30 min. Next, 15 g flaky aluminium with 40 mL anhydrous ethanol was added to a 250 mL three-neck flask. The dispersed GO mixture was added and mixed at 50°C. TEOS (12.5 g) in 20 mL anhydrous ethanol and ammonia (3 g) in 20 mL anhydrous ethanol were added into the flask with constant pressure droplet funnel simultaneously for 30 min. The reaction was carried out at 50°C for 4.5 h. After the reaction, the product was filtered and washed with anhydrous ethanol three times and cleaned with acetone twice, and then dried in a vacuum oven at 25°C. In the meantime, SEWFA was also prepared according to the above method only without GO for comparison.

2.3. Characterisation: The microstructure of the GO-SEWFA was assessed by scanning electron microscopy (SEM) (JEOL JSM-7500F) operated at 15.0 kV and elemental surface composition was studied with energy-dispersive X-ray spectroscopy (EDS) (Philips XL30).

3. Results and discussion

3.1. SEWFA modified with GO: GO retains a two-dimensional (2D) layer structure, and its surface has abundant oxygen-containing groups such as hydroxyl (-OH), epoxy (C-O-C), carbonyl (C = O) and carboxyl groups (-COOH). GO can react with other reagents or polymers containing active groups, and give it good dispersion in a matrix or water solution [17]. Few-layer GO was successfully prepared (Figs. 5 and 7), which was rich in oxygen-containing active groups at a carbon-oxygen ratio of 1.66 (Fig. 6).

During the encapsulation process, alkali was chosen as the catalyst, the resulting film becomes dense and continuous because of the condensed silica forms a 3D network structure [18, 19]. After GO was added to the encapsulating solution, the oxygen-containing groups on the GO sheets, such as hydroxyl and carboxyl groups, could participate in the condensation reaction of TEOS during the encapsulating process, and the GO could also be introduced into the silica-based encapsulating film. From Fig. 1, the hydrolysis and polycondensation of TEOS were simultaneously carried out. The polycondensation product (Si-O-Si) could develop into a 3D fully formed network structure. At the same time, they should

doi: 10.1049/mnl.2020.0268

also react with active groups of GO and Si-OH to form a layer of silica-based composite films encapsulated on flaky aluminium. All the hypothetical modifications above-mentioned will be confirmed by the improved initial hydrogen evolution results.

3.2. Anticorrosive performance of GO-SEWFA: The anticorrosive performance of GO-SEWFA and SEWFA can be characterised by monitoring hydrogen evolution in dilute HCl [19]. Fig. 2*a* is the test setup for hydrogen evolution. Both SEWFA and GO-SEWFA (0.5 g) were separately put in 100 mL dilute HCl (0.1 mol/L) in a dry filter flask. Evolved hydrogen was captured and measured every 10 min for 630 min, and the hydrogen evolution results are shown in Fig. 2*b*. Both samples produced hydrogen soon after immersion, indicating that both GO-SEWFA and SEWFA have good wettability. The two curves have the same shape with slow hydrogen evolution at the beginning, and then hydrogen evolution accelerates as the immersion time increases, eventually reaching equilibrium. However, the hydrogen evolution of GO-SEWFA is obviously slower than that of SEWFA from the beginning to 130 min, and the amount of hydrogen evolution of GO-SEWFA is a little lower than that of SEWFA after 630 min. Based on the initial hydrogen evolution between GO-SEWFA and SEWFA, it is demonstrated that the anticorrosive performance of SEWFA is improved by encapsulating the GO/silica matrix.

3.3. Morphology of GO-SEWFA: The GO-SEWFA morphology was imaged using SEM. As seen in Fig. 3*a*, GO is distributed on the surface of GO-SEWFA, showing clear nanosheets contour shape. There is no obvious agglomeration between GO nanosheets in the silica-based matrix. At higher magnification of SEM (Fig. 3*b*), the GO-SEWFA morphology shows many bright spots attached to GO, which should be silica nanoparticles, the hydrolysis and polycondensation product of TEOS. The element mapping images of Al and C demonstrate that Al and C elements appear

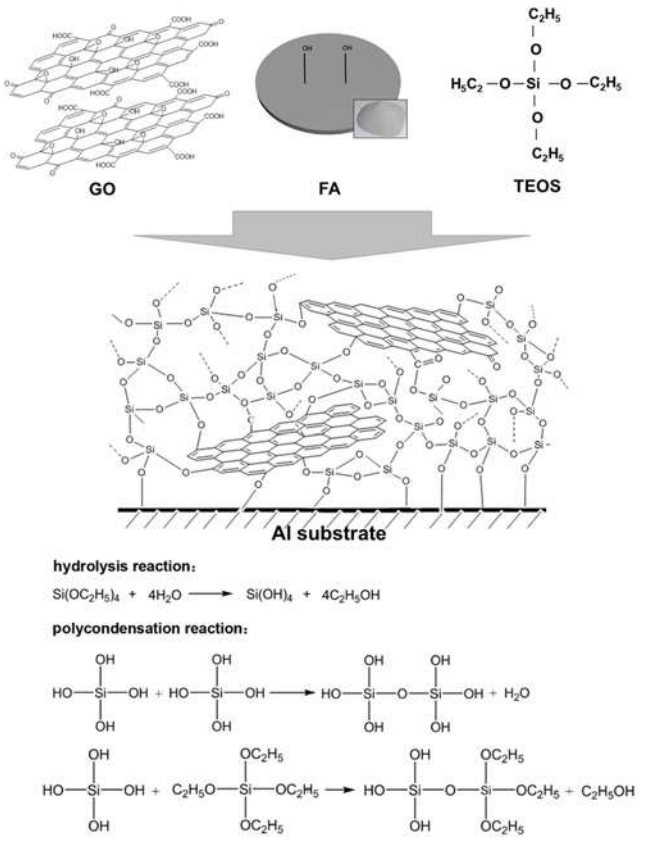

Fig. 1 *Illustrative diagram of the chemical reaction and network structure of GO-SEWFA*

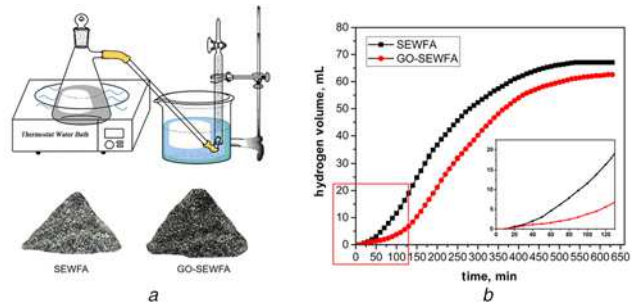

Fig. 2 *Hydrogen evolution of SEWFA and GO-SEWFA*
a Testing device and samples
b Hydrogen evolution at different times

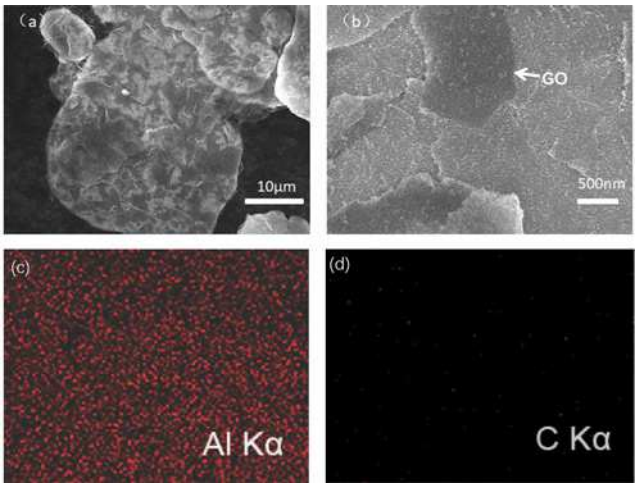

Fig. 3 *SEM images of GO-SEWFA and EDS elemental maps of GO area*
a SEM image of GO-SEWFA
b SEM image of enlarged GO-SEWFA
c EDS elemental map of Al
d EDS elemental maps of C

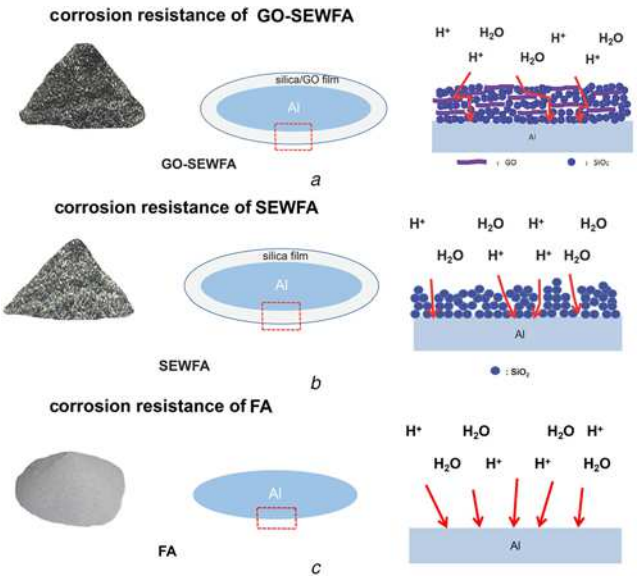

Fig. 4 *The structure and their schematic diagram of corrosion resistance*
a GO-SEWFA
b SEWFA
c FA

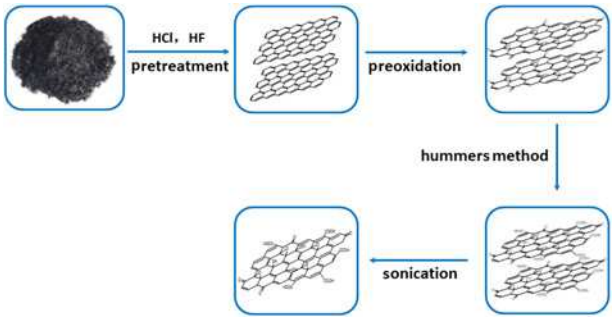

Fig. 5 *Synthetic route used to obtain GO*

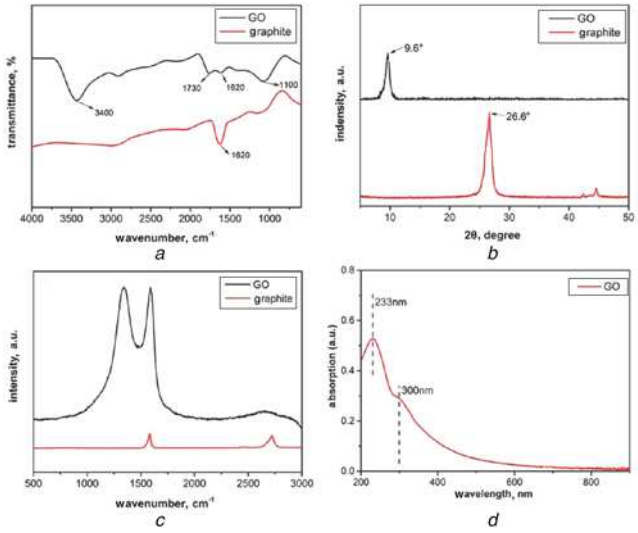

Fig. 6 *The instrumental analysis results of GO*
a FT-IR spectra
b Raman spectra
c XRD of GO and graphite
d UV–Vis spectra of GO samples

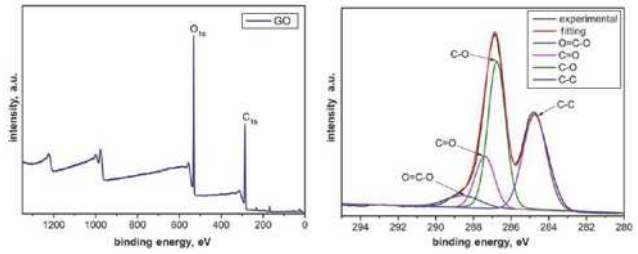

Fig. 7 *XPS spectra and C_{1s} spectra of GO*

on the surface of GO-SEWFA in Figs. 3*c* and *d*, and the quantitative results of the Si/C element ratio is 2.51. Al displays intense signal, while C is weak signals, all scattered with few colour dots. It can be inferred from SEM and EDS that the encapsulating film is thin, GO and silica form an intimate hybrid in the matrix structure, which is the same as higher extent of Si-O-Si condensation reaction in silane coating by adding functionalised GO [20].

The difference in corrosion resistance between SEWFA and GO-SEWFA is due to the different structure of the coated film on the surface of flaky aluminium. Here, the application of GO has similar mechanism with its use in corrosion-resistance coatings [21, 22]. In the structure of the encapsulated film of GO-SEWFA, silica acts as a shielding and supporting structure similar to the matrix, while each GO sheet acts mainly as a flaky barrier material, which can effectively prevent the penetration of corrosion media by spreading along the surface of flaky aluminium and make it have a strong shielding effect (Fig. 4). It solves basically the agglomeration phenomenon of GO in the practical application. Therefore, the corrosion resistance of GO-SEWFA is better than that of SEWFA. GO-SEWFA with enhanced anticorrosive property is beneficial to its use in industrial fields, especially for the corrosion-resistance coatings.

4. Conclusion: GO was used to modify SEWFA to improve its anticorrosive properties, and the GO/silica hybrid film showed a lower initial hydrogen evolution in dilute HCl. SEM and EDS results supported that the flaky aluminium was successfully covered by composite silica-based film with GO, and the GO and silica formed a 3D network structure. This new SEWFA with enhanced anticorrosive property is a promising functional material, which could be preferred under certain requirements in industrial application due to solve the agglomeration of GO basically by the formation of silica/GO matrix.

5. Acknowledgment: This work was supported by the National Major Science and Technology Projects of China (grant 2017YFB0309700).

6 References

[1] Ma Z., Qiao Y., Xie F., *ET AL.*: 'Effect of preparation temperature on the corrosion resistance of waterborne aluminium pigments', *Pigm. Resin Technol.*, 2017, **46**, (3), pp. 203–209
[2] Wang K., Wang C., Yin Y., *ET AL.*: 'Modification of Al pigment with graphene for infrared/visual stealth compatible fabric coating', *J. Alloys Compd.*, 2017, **690**, pp. 741–748
[3] Niroumandrad S., Rostami M., Ramezanzadeh B.: 'Corrosion resistance of flaky aluminium pigment coated with cerium oxides/hydroxides in chloride and acidic electrolytes', *Appl. Surf. Sci.*, 2015, **357**, pp. 2121–2130
[4] Zhu W., Li W., Mu S., *ET AL.*: 'Comparative study on Ti/Zr/V and chromate conversion treated aluminum alloys: anti-corrosion performance and epoxy coating adhesion properties', *Appl. Surf. Sci.*, 2017, **405**, pp. 157–168
[5] Hartl H., Guo Y., Ostrikov K., *ET AL.*: 'Film formation from plasma-enabled surface-catalyzed dehalogenative coupling of a small organic molecule', *RSC Adv.*, 2019, **9**, (5), pp. 2848–2856
[6] Pi P., Liu C., Wen X., *ET AL.*: 'Improved performance of aluminium pigments encapsulated in hybrid inorganic-organic films', *Particuology*, 2015, **19**, pp. 93–98
[7] Wang Y., Gu Z., Liu J., *ET AL.*: 'An organic/inorganic composite multi-layer coating to improve the corrosion resistance of AZ31B Mg alloy', *Surf. Coat. Tech.*, 2019, **360**, pp. 276–284
[8] Ma Z, Qiao Y., Wen Y., *ET AL.*: 'Effect of precursors on the anti-corrosion property of silica encapsulated waterborne aluminium pigments', *Pigm. Resin Technol.*, 2017, **46**, (2), pp. 100–106
[9] Tawiah B., Zhang L., Tian A., *ET AL.*: 'Coloration of aluminium pigment using SiO2 and γ-glycidoxypropyltrimethoxysilane with dichlorotriazine reactive dye', *Pigm. Resin Technol.*, 2016, **45**, pp. 335–345
[10] Ma Z.L., Li C.C., Wei H.M., *ET AL.*: 'Silica sol-gel anchoring on aluminium pigments surface for corrosion resistance based on aluminium oxidized by hydrogen peroxide', *Dyes Pigm.*, 2015, **114**, pp. 253–258
[11] Kiehl A., Brendel H.: 'Corrosion inhibited metal pigments', *Macromol. Symp.*, 2002, **187**, pp. 109–120
[12] Jiang F., Zhao W., Wu Y., *ET AL.*: 'Anti-corrosion behaviors of epoxy composite coatings enhanced via graphene oxide with different aspect ratios', *Prog. Org. Coat.*, 2019, **127**, pp. 70–79
[13] Wang J., Lei W., Deng Y., *ET AL.*: 'Effect of current density on microstructure and corrosion resistance of Ni-graphene oxide composite coating electrodeposited under supercritical carbon dioxide', *Surf. Coat. Tech.*, 2019, **358**, pp. 765–774
[14] Ye Y., Zhang D., Li J., *ET AL.*: 'One-step synthesis of superhydrophobic polyhedral oligomeric silsesquioxane-graphene oxide and its application in anti-corrosion and anti-wear fields', *Corros. Sci.*, 2019, **147**, pp. 9–21

doi: 10.1049/mnl.2020.0268

[15] Laleh R.R., Savaloni H., Abdi F., *ET AL.*: 'Corrosion inhibition enhancement of Al alloy by graphene oxide coating in NaCl solution', *Prog. Org. Coat.*, 2019, **127**, pp. 300–307
[16] Dun Y., Zhao X., Tang Y., *ET AL.*: 'Microstructure and corrosion resistance of a fluorosilane modified silane-graphene film on 2024 aluminum alloy', *Appl. Surf. Sci.*, 2018, **437**, pp. 152–160
[17] Marcano D.C., Kosynkin D.V., Berlin J.M., *ET AL.*: 'Improved synthesis of graphene oxide', *ACS Nano*, 2010, **4**, pp. 4806–4814
[18] Baig N., Chauhan D.S., Sale T.A., *ET AL.*: 'Diethylenetriamine functionalized graphene oxide as a novel corrosion inhibitor for mild steel in hydrochloric acid solutions', *New J. Chem.*, 2019, **43**, (5), pp. 2328–2337
[19] He L.H., Zhao Y., Xing L.Y., *ET AL.*: 'Preparation of phosphonic acid functionalized graphene oxide-modified aluminum powder with enhanced anticorrosive properties', *Appl. Sur. Sci.*, 2017, **411**, pp. 235–239
[20] Ahmadi A., Ramezanzadeh B., Mahdavian M.: 'Hybrid silane coating reinforced with silanized graphene oxide nanosheets with improved corrosion protective performance', *RSC Adv.*, 2016, **6**, pp. 54102–54112
[21] Kumar S.K., Castro M., Saiter A., *ET AL.*: 'Development of poly (isobutylene-coisoprene) reduced graphene oxide nanocomposites for barrier, dielectric and sensing applications', *Mater. Lett.*, 2013, **96**, pp. 109–112
[22] Yu Z., Di H., Ma Y., *ET AL.*: 'Fabrication of graphene oxide–alumina hybrids to reinforce the anti-corrosion performance of composite epoxy coatings', *Appl. Surf. Sci.*, 2015, **351**, pp. 986–996
[23] Yu Z.Z., Di H., Ma Y., *ET AL.*: 'Raphene oxide–alumina hybrids to reinforce the anti-corrosion performance of composite epoxy coatings', *Appl. Surf. Sci.*, 2015, **351**, pp. 986–996
[24] Dedkov Y.S., Fonin M., Laubschat C.: 'A possible source of spin-polarized electrons: the inert graphene/Ni(111) system', *Appl. Phys. Lett.*, 2008, **92**, p. 052506
[25] Du B., Zhou S.S., Li N.L., *ET AL.*: 'Research progress of surface modification of aluminium powders for corrosion protection', *Appl. Mech. Mater.*, 2011, **80–81**, pp. 70–75

7. Appendix: GO prepared with the improved Hummer's method

7.1. Experimental details

7.1.1. Materials: Graphite powder (99.95%, 325 mesh) was provided by McLean Biochemical Technology Co., Ltd. (Shanghai, China). 98% H_2SO_4, HF, $KMnO_4$, $NaNO_3$, HCl, H_2O_2, P_2O_5, $K_2S_2O_8$ were of analytical reagent and provided by Sinopharm Group Chemical Reagent Co., Ltd. Flaky aluminium powder was provided by Pancai Metal Pigment Co., Ltd. TEOS was provided by Jiuhuan New Materials Technology Co., Ltd.

7.1.2. Preparation of GO: Graphite was pretreated with dilute HCl (5%) and HF (5%) at room temperature, followed by pre-oxidation with $K_2S_2O_8$, P_2O_5 and H_2SO_4 at 80°C. Using a three-stage improved Hummer's method, pre-treated graphite was subjected to an initial low-temperature intercalation, followed by medium-temperature oxidation, and a final high-temperature hydrolysis [14]. The synthetic route is illustrated in Fig. 5. A series of reactions were carried out with 3 g of graphite, 69 mL of H_2SO_4, 1.5 g of $NaNO_3$ and 12 g of $KMnO_4$.

7.1.3. Characterisation: GO samples were characterised by Fourier-transform infrared spectroscopy (FT-IR) (Nicolet 380) and Raman spectroscopy (INVIA). Binding energies relative coverage for oxygen-containing functional group species were measured with X-ray photoelectron spectroscopy (XPS) (ESCALAB 250Xi). Field emission transmission electron microscopy (JEOL JEM-2100F) and selected area electron diffraction (SAED) patterns were used to study the morphology of GO. Phase information and comparisons between graphite and GO were collected using X-ray diffraction (XRD) (D/MAX2200).

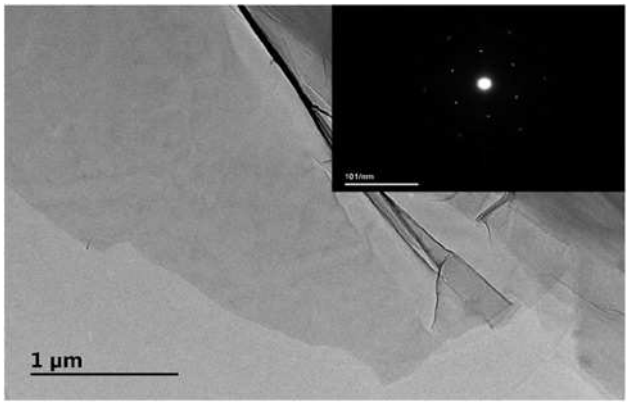

Fig. 8 *TEM image of GO; the insert shows the corresponding SAED pattern*

7.2. Results and discussion: The oxygen-containing groups in GO were confirmed by FT-IR. As shown in Fig. 6*a*, several peaks appear in the spectrum compared with graphite. Peaks at 3400, 1730, 1620 and 1100 cm^{-1} were attributed to the stretching vibrations of -OH, C = O, C = C and C-O-C, respectively [23–25]. Compared with graphite, GO contains hydroxyl (-OH), epoxy (C-O-C), carboxyl (-COOH) and carbonyl (C = O) groups to support successful preparation of GO initially.

Raman spectra were collected of the prepared samples to further characterise GO. For GO and graphite (Fig. 6*b*), there are two bands centered at 1345 and 1580 cm^{-1}, which were attributed to the D-band and G-band, respectively. The D-band correlates with the degree of disorder. Compared with graphite, GO has a higher D-band, indicating that the original graphite structure was disordered during the oxidation process [12]. Diffraction data also shows dramatic differences in graphite and GO (Fig. 6*c*). GO shows a diffraction peak at $2\theta = 9.6°$ corresponding to a lattice spacing of $d = 0.914$ nm, and the graphite peak at $2\theta = 26.6°$ disappears, indicating that the graphite has been oxidised. The interlayer spacing of GO is increased due to the introduction of the oxygen-containing groups. Although oxidation introduces a variety of oxygen-containing groups, the GO still maintains a crystalline structure with a relatively sharp and weak diffraction peak.

UV–Vis results in Fig. 6*d* show two absorption features with a strong absorption peak at 233 nm that corresponds to the π–π* transition of C = C bond, while the shoulder at 300 nm corresponds to the n–π* transition of the C = O bond. XPS was used to measure the C/O ratio and degree of oxidation, as well as to quantify the different oxygen-containing groups.

The XPS survey spectra of GO and the C_{1s} scan are shown in Fig. 7. GO was chosen as the precursor to modify the SEWFA at a carbon-oxygen ratio of 1.66. The morphology of the GO was observed by TEM, as shown in Fig. 8. The sheet was several micrometers in layer dimension with a thin-layer structure and wrinkled surface texture. Simultaneously, the SAED pattern of GO shows well-defined six-fold symmetric diffraction spots.